STUDIA UBB CHEMIA, LXII, 1, 2017 (p. 203-212)
(RECOMMENDED CITATION)
DOI:10.24193/subbchem.2017.1.18

PREPARATION, CHARACTERIZATION, AND EVALUATION OF THE PHOTOCATALYTIC EFFECT OF α-Fe_2O_3/SAPO-34 IN THE ELIMINATION PROCESS OF THE ANTI-CANCER DRUG DOXORUBICIN FROM AQUEOUS SOLUTION

MOHAMMAD HOSEIN BIGTAN[a] AND KAZEM MAHANPOOR[a]*

ABSTRACT. In this investigation, α-Fe_2O_3/SAPO-34 nano-structure were synthesized and characterized by XRD, SEM and FT-IR techniques. Morphologically, the shape of α-Fe_2O_3/SAPO-34 nanoparticles is close to spherical nanoparticles with an average particle size of 93 nm determined by Debye-Scherrer equation. The photocatalytic activity of α-Fe_2O_3/SAPO-34 nano-structure was investigated through the degradation of doxorubicin, an anti-cancer drug using a batch reactor under UV-C irradiation and H_2O_2 as oxidant. The effect of various factors including drug concentration, catalyst dosage, pH and H_2O_2 concentration on the degradation yield were investigated. The results showed that optimum conditions were: Initial concentration of DOX = 20 ppm, pH = 8, amount of α-Fe_2O_3/SAPO-34 = 150 mg/L, and H_2O_2 concentration 4 mol/L.

Keywords: *Doxorubicin, Photocatalytic degradation, α-Fe_2O_3/SAPO-34, Nanocatalyst*

INTRODUCTION

Adriamycin is a trade name for Doxorubicin (DOX) which is an anthracycline antitumor antibiotic. DOX has been synthesized via biotechnological methods [1]. DOX is applied in the treatment of various cancers such as bladder, stomach, breast, ovaries, lung, thyroid, multiple myeloma, soft tissue sarcoma, leukemia, Hodgkin's lymphoma and other kinds of cancers [2]. In the pharmaceutical industry, this drug can be excreted into the environment through production excretion, formulation sites, as well as un-metabolised substances or their metabolites in urine or stool of the direct consumers of the

[a] *Department of Chemistry, Arak Branch, Islamic Azad University, Arak, Iran; Tel. +98-86-33422226; Fax. +98-86-33470017.*
* *Corresponding author: k.mahanpoor@gmail.com, k-mahanpoor@iau-arak.ac.ir*

drug [3]. So due to the high toxicity of this drug, it should be completely degraded before entering the environment. To remove the anti-cancer drugs, several methods have been reported such as using a membrane, activated carbon adsorption, electrolysis, sonolysis and ozonation [4–7]. Since conventional treatments are often inadequate and inefficient to remove DOX and other pharmaceuticals from wastewater [8], further investigations on alternative treatment options are intensively pursued. Advanced oxidation processes (AOPs) as an appropriate alternative can act about biological wastewater treatments, as a pre-treatment, enhancing the biodegradability by partial oxidation or can be used as a post-treatment to degrade persistent compounds [9]. Among the AOP's, heterogeneous photocatalytic oxidation has shown high efficiency in the treatment of industrial wastewaters, ground waters and contaminated air [10].

In this study, α-Fe_2O_3 nanostructure was supported on porous SAPO-34 to increase its photocatalytic activity. Photocatalytic properties of α-Fe_2O_3/SAPO-34 on removing the anti-cancer drug, DOX were evaluated, and operational parameters were considered and optimized.

RESULTS AND DISCUSSION

As it could be seen in Figure 1, the XRD patterns of SAPO-34 (catalyst support) and α-Fe_2O_3/SAPO-34 were showed the interaction between α-Fe_2O_3 and SAPO-34. As observed in the XRD pattern of α-Fe_2O_3/SAPO-34, the SAPO-34 frame structure has not being destroyed after α-Fe_2O_3 loading. An average particle size of 93 nm for α-Fe_2O_3/SAPO-34 particles was obtained by employing the Debye-Scherrer equation.

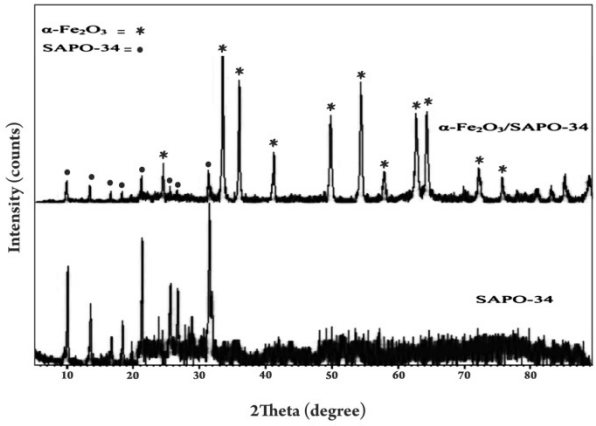

Figure 1. XRD powder patterns of α-Fe_2O_3/SAPO-34 and SAPO-34 as a catalyst support

As it is evident in Figure 2, the size of iron oxide nanoparticles supporting on SAPO-34 is not quite the same, and their distribution is not uniform. Non-Uniformity of the catalyst surface confirms that the photocatalytic activity of these nanoparticles is increased. Morphologically, the shape of α-Fe_2O_3/SAPO-34 nanoparticles is close to spherical nanoparticles.

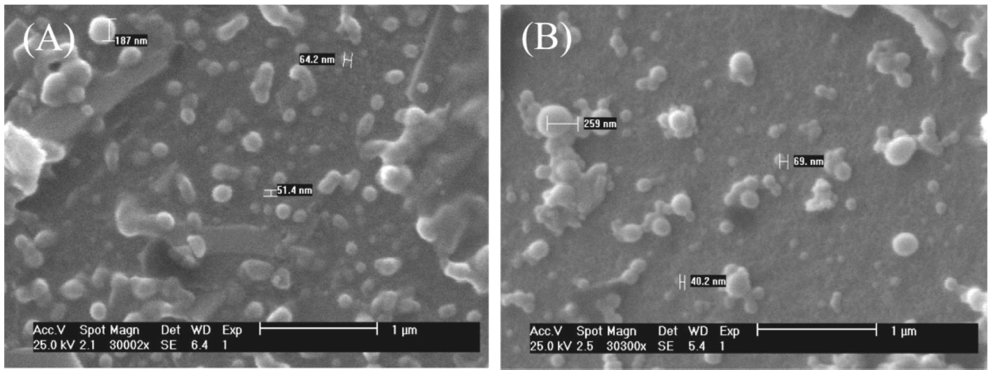

Figure 2. SEM images of α-Fe_2O_3/SAPO-34 nanoparticles (A) and SAPO-34 (B)

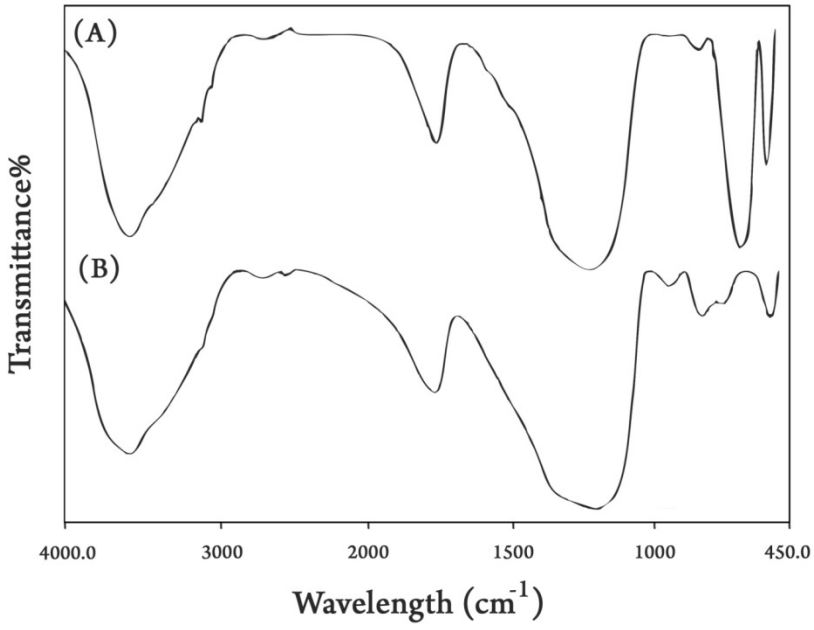

Figure 3. FTIR spectra of α-Fe_2O_3/SAPO-34 (A), catalyst support of SAPO-34(B)

Figure 3 illustrates the FTIR spectra of the synthesized catalysts. In the primary spectra of SAPO-34 catalyst support (Figure 3A), the bending around 520 cm^{-1} is the signature of SiO_4 that attributes to Si which incorporated to the tetragonal structure of SAPO-34. The peaks at wave numbers about 780, 1100 and 1650 cm^{-1} belong to the asymmetric stretch of O–P–O, symmetric stretch of O–P–O and physically adsorbed water, respectively. The peak at 3440 Cm^{-1} ascribed to the structural OH [11]. This peak includes P–OH, Si–OH, Al–OH and Si–OH–Al bonds which are active sites in the cages of SAPO-34. In the FTIR spectra of the nano photocatalyst α-Fe_2O_3/SAPO-34 (Figure 3B), the peaks at about 3430 and 1640 cm^{-1} are assigned to stretching and bending modes of OH. The peak at about 720 cm^{-1} ascribed to the Fe-O bond [12]. Other Spectral changes between 450 and 700 cm^{-1} imply the formation of new bonds between α-Fe_2O_3 and SAPO-34.

Photocatalytic degradation investigation of DOX

Hematite is an *n*-type semiconductor with the band gap of 2.2 eV, the conduction band edge at +0.28 V and the valance band edge at +2.4 eV [13]. This photocatalytic process is based on the adsorption and desorption of molecules on the catalyst surface. The UV light irradiation to the porous α-Fe_2O_3/SAPO-34 causes the valence band (VB) electrons to eject into the conduction band (CB), so holes are generated in the valence band. The photogenerated holes undergo a reaction with adsorbed water on the surface of the catalyst to produce the highly reactive hydroxyl radical ($^{\bullet}OH$). On the other hand, a superoxide anion radical ($O_2^{\bullet -}$) is produced since O_2 is an electron acceptor. Moreover, $O_2^{\bullet -}$ acts as an oxidizing agent or an additional source of $^{\bullet}OH$. The high oxidative potential of these reactive radicals degrades DOX drug into non-toxic organic compounds. So stabilization of α-Fe_2O_3 on SAPO-34 catalyst support leads to increase the photocatalytic activity. The increase of photocatalytic activity is due to the suitable position of SAPO-34 for adsorption of DOX in the vicinity of α-Fe_2O_3 which is the producer of reactive hydroxyl radical ($^{\bullet}OH$).

The effect of initial DOX concentration on photodegradation efficiency is shown in Figure 4. It was observed that the photodegradation conversion of DOX decreases when the initial concentration of DOX is increased. The probable reason is that when the initial concentration of DOX is increased, more and more DOX molecules are adsorbed on the surface of α-Fe_2O_3/SAPO-34. A significant amount of adsorbed DOX is thought to have an inhibitive effect on the reaction of DOX molecules with photogenerated holes or hydroxyl radicals, because of the lack of direct contact between them. Once the concentration of DOX is increased, it also causes the DOX molecules to absorb light, and the photons never reach the photocatalyst surface. Thus the photodegradation efficiency decreases.

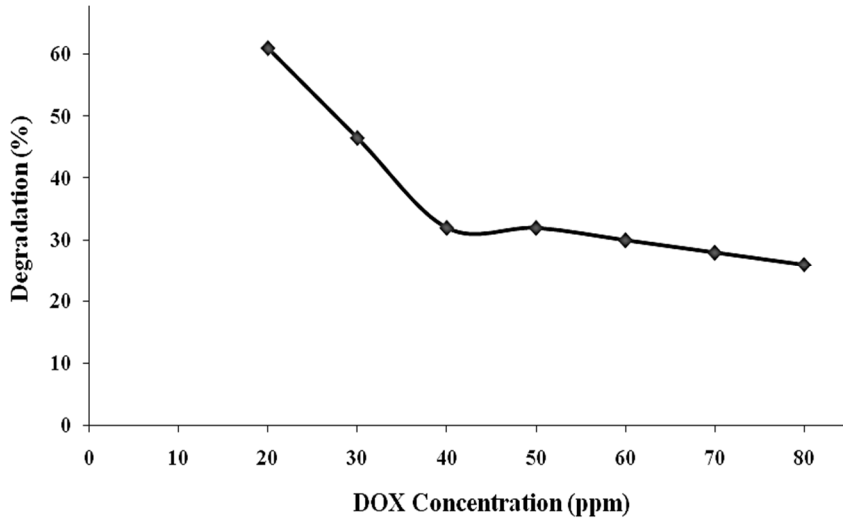

Figure 4. Effect of initial DOX concentration on photo degradation efficiency (α-Fe_2O_3/SAPO-34 = 400 mg/L, initial pH = 5; irradiation time = 120 min)

Figure 5 shows the amount of α-Fe_2O_3/SAPO-34 nano photocatalyst on DOX degradation in a constant initial concentration (20 ppm), pH = 5, and the irradiation time of 120 min. By increasing the amount of the catalyst up to 150 mg, degradation increases. The further increase of the catalyst leads to a decrease in degradation. Based on the observations, the optimized value of the catalyst loading is about 15 mg under the given experimental condition. The pollutant degradation improvement because of photocatalytic loading is because of the access to the total surface area and active sites of the catalyst. The observed decrease in degradation efficiency, by using an excess amount of the catalyst, is a result of the created opacity in high concentrations of the photocatalyst.

As it can be seen in Figure 6, in alkaline media, the possibility of $^{\bullet}OH$ radicals generation increases as the result of the reaction between hydroxyl ions (OH^-) and produced holes in the valence band. Generating higher amounts of $^{\bullet}OH$ radicals, leads to more radical attacks to DOX molecules, so the process efficiency increases. Furthermore, due to the structure of DOX molecule, the presence of the OH groups attached to the benzene ring and hydroxyl groups with acidic hydrogen (because of the high polarity of OH) can lose hydrogen in an alkali media followed by the formation of negatively charged oxygen in the molecule. Since the catalyst surface is acidic, the adsorption capability of DOX onto catalyst increases and so $^{\bullet}OH$ radicals attack the adsorbed DOX molecules more and the process efficiency increases.

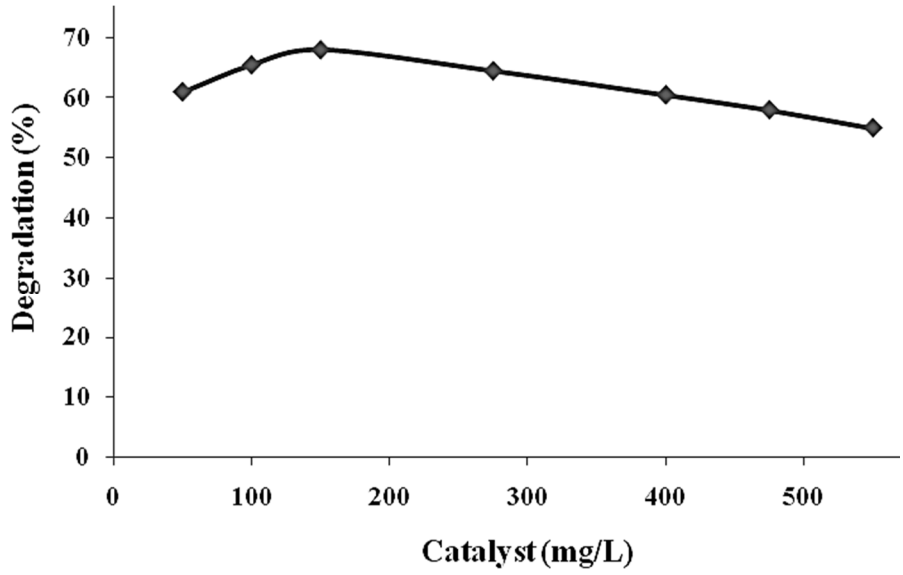

Figure 5. The effect of the amount of α-Fe_2O_3/SAPO-34 on photodegradation efficiency of DOX (Initial concentration of DOX = 20 ppm, pH= 5; irradiation time = 120 min)

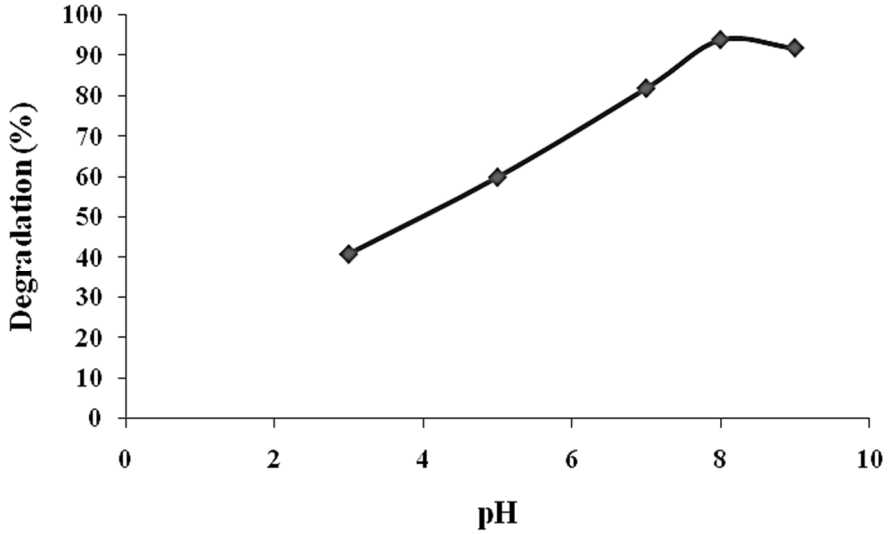

Figure 6. Effect of pH value on photodegradation efficiency of DOX at the irradiation time of 120 min (Initial concentration of DOX = 20 ppm, α-Fe_2O_3/SAPO-34 = 150 mg/L)

H_2O_2 is an electron scavenger which accepts photogenerated electrons from the conduction band and prevents the electron-hole recombination to generate hydroxyl radicals (•OH) [14]. The photo-catalytic degradation of DOX was performed at different concentrations of hydrogen peroxide and in the presence of an optimized amount of other laboratory factors. The results are shown in Figure 7. By increasing H_2O_2 concentration up to 4 mol/L, the complete degradation of DOX occurs in a short time (30 min). Degradation efficiency enhancement by increasing the amount of H_2O_2 could be attributed to increasing the concentration of reactive hydroxyl radicals (1). Moreover, by light radiation, the hydrogen peroxide molecule undergoes a cleavage to produce O_2 gas (2). According to the photocatalytic mechanism, the O_2 gas reacts with conduction band electrons through several steps and generates •OH radicals (3-5).

$$e_{CB}^{-} + H_2O_2 \rightarrow OH^{-} + {}^{\bullet}OH \quad (1)$$

$$2\,H_2O_2 \xrightarrow{h\nu} O_2\uparrow + 2\,H_2O \quad (2)$$

$$O_2\uparrow + e_{CB}^{-} \rightarrow O_2^{\bullet -} \quad (3)$$

$$O_2^{\bullet -} + 2H^{+} + e_{CB}^{-} \rightarrow H_2O_2 \quad (4)$$

$$H_2O_2 + H^{+} + e_{CB}^{-} \rightarrow {}^{\bullet}OH + H_2O \quad (5)$$

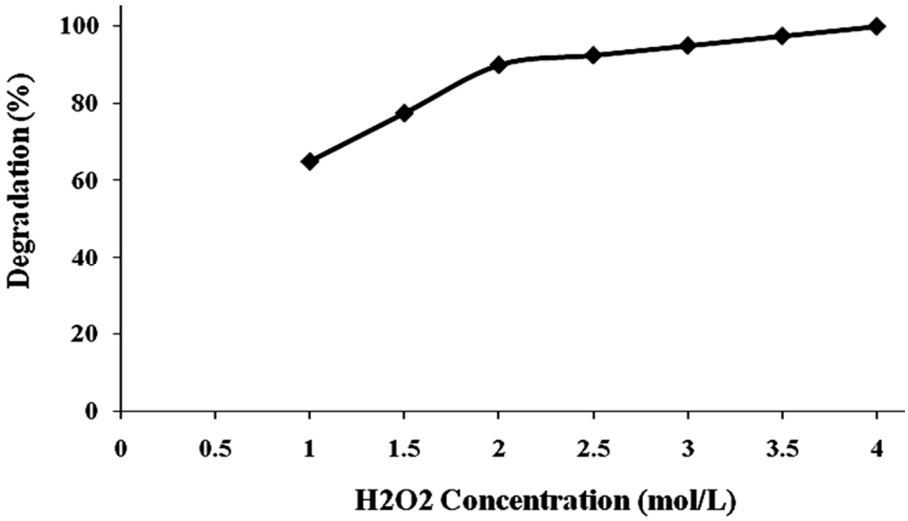

Figure 7. Effect of H_2O_2 concentration on DOX degradation after 30 min in UV/α-Fe_2O_3/SAPO-34 process (Initial concentration of DOX = 20 ppm, pH = 8, amount of α-Fe_2O_3/SAPO-34 = 150 mg/L)

CONCLUSIONS

The α-Fe_2O_3/SAPO-34 nanostructure was prepared by encapsulation of α-Fe_2O_3 with SAPO-34 and was characterized by XRD, SEM and FT-IR techniques. Next, the photocatalytic degradation removal of DOX through advanced oxidation processes (AOP) has been studied under basic conditions using UV/α-Fe_2O_3/SAPO-34/H_2O_2 system. The results obtained showed that the photocatalytic degradation of DOX decreases with an increase in the concentration of DOX. The effect of initial DOX concentration, catalyst dosage, pH and H_2O_2 concentration on the photocatalytic of DOX were investigated. Finally, the optimum condition were determined as Initial concentration of DOX = 20 ppm, pH = 8, amount of α-Fe_2O_3/SAPO-34 = 150 mg/L, and H_2O_2 concentration 4 mol/L. Using α-Fe_2O_3/SAPO-34 nano photocatalyst at different alkaline pHs can be a logical economic and scientific solution for the treatment of wastewaters containing this anticancer drug. This work suggested that the α-Fe_2O_3/SAPO-34 nanostructures could be regarded as a prominent catalyst for the degradation of drugs under mild conditions. It is hoped that the present survey opens a new window of magnetically catalysts to be used as a photocatalyst in the field of drug degradation.

EXPERIMENTAL SECTION

Iron(III) chloride hexahydrate was purchased from Daejung Company (Korea). Fumed silica was purchased from Sigma-Aldrich (USA). Aluminum isopropoxide and cyclohexylamine were purchased from Titrachem Company (Iran). Hydrogen peroxide (30%) was purchased from Chem Lab Company (Belgium). Other reagents such as Urea, orthophosphoric acid, ethanol (96%), sodium hydroxide and sulfuric acid (95-97%) were purchased from Merck (Germany). DOX was purchased from RPG Life Sciences Limited (Mumbai, India). The absorbance measurements were taken on a Perkin Elmer Lambda 25 UV/Vis spectrophotometer using silica cells with a path length of 10 mm. The surface morphology of the catalyst was analyzed using scanning electron microscopy (SEM) on a Philips XL 30 microscope. X-ray powder diffraction patterns were recorded using a Cu radiation (λ= 1.5406) source on a Philips PW 1800 X-ray diffractometer. Fourier transform infrared spectroscopy (FT-IR) was carried out on a Perkin Elmer Spectrum 400 spectrophotometer using a KBr pallet for sample preparation. The solutions pH values were measured on a Metrohm 780 pH meter.

Preparation of α-Fe_2O_3 nano-particles

α-Fe_2O_3 nanoparticles were synthesized according to the procedure reported by Chaudhari *et-al.* [15] as follow: a solution of ferric chloride hexahydrate (0.25 mol in 1L of water) was mixed with a solution of urea (1 M) and the mixture was magnetically stirred for 30 min and subsequently refluxed for 12 hours. The precipitate was filtered, washed with 100 mL of aqueous ethanol, dried at 80 °C for 2 hours and calcinated at 300 °C for 1 hour to obtain the hematite as yellowish brown powder.

Preparation of SAPO-34

a mixture of Aluminum isopropoxide (6.8 g) and Orthophosphoric acid (3.3 g) was dissolved in deionised water (14 g) and vigorously stirred for 1 hour. Subsequently, an aqueous solution of Cyclohexylamine (9.9% w/w) was added to the mixture and stirred for another 1 hour. The resultany mixture was combined with fumed Silica (0.96 g) and the solution was allowed to be stirred for 2 hours, until a gel was formed. Next, the synthesized gel was transferred into a 60 mL stainless steel autoclave and kept at 200 °C for 24 hours. The obtained product was filtered and washed with water, dried at room temperature and calcinated at 550 °C for 20 hours [16].

Preparation of α-Fe_2O_3/SAPO-34 nano photocatalyst

To a mixture of SAPO-34 and α-Fe_2O_3 with the weight ratio of 3:1, ethanol was added dropwise to obtain a mud-like shape. The obtained mixture was dried at 80 °C for 2 hours and calcinated at 300 °C for 1 hour to get the yellowish brown powder. [18].

The photocatalytic activity of α-Fe_2O_3/SAPO-34

Typical procedure: A batch reactor amended with three Philips lamps (15 W, UV- C) was used to investigate the photocatalytic activity of α-Fe_2O_3/SAPO-34. 20 mL of each DOX solution (20 ppm) was inserted into 100 mL glass beaker. Catalyst with the concentration of 150 mg/L was added to the beaker. The pH of the solution was adjusted to 8 using NaOH solution. The mixture was stirred at dark for 15 min to establish adsorption-desorption equilibrium. The solution was then exposed to the bach reactor for variable time intervals (10 min). At each time interval, about 3.0 mL of the suspension was collected after centrifugation to remove the photocatalyst particles and was quickly subjected to concentration measurement using a UV-1780 UV–vis spectrophotometer (Shimadzu, Japan) at room temperature.

The efficiency of degradation was calculated using the formula: Degradation% = $(A_0-A_t)/A_0$, where A_0 is the initial absorption of the sample and A_t is the absorption through the t sampling time.

ACKNOWLEDGMENTS

The authors are thankful to Islamic Azad University, Arak Branch for the preparation of experimental setup.

REFERENCES

1. A. Grimm, K. Madduri, A. Ali, C.R. Hutchinson, *Gene*, **1994**, *151*, 1.
2. A. Brayfield, ed. "Doxorubicin". Martindale: The Complete Drug Reference. Pharmaceutical Press, **2013**.
3. S.N. Mahnik, K. Lenz, N. Weissenbacher, R.M. Mader, M. Fuerhacker, *Chemosphere,* **2007**, *66*, 30.
4. Z. Chen, G. Park, P. Herckes, P. Westerhoff, *J. Adv. Oxid. Technol.*, **2008**, *11*, 254.
5. J. Hirose, F. Kondo, T. Nakano, T. Kobayashi, N. Hiro, Y. Ando, H. Takenaka, K. Sano, *Chemosphere*, **2005**, *60*, 1018.
6. C.A. Somensi, E.L. Simionatto, J.B. Dalmarco, P. Gaspareto, C.M. Radetski, *J. Environ. Sci. Health A.*, **2012**, *47*, 1543.
7. X.H. Wang, A.Y.C. Lin, *Environ. Pollut.,* **2014**, *186*, 203.
8. N. De la Cruz, J. Giménez, S. Esplugas, D. Grandjean, L.F. De Alencastro, C. Pulgarín, *Water Res.*, **2012**, *46*, 1947.
9. A. Chatzitakis, C. Berberidou, I. Paspaltsis, G. Kyriakou, T. Sklaviadis, I. Poulios, *Water Res.*, **2008**, *42*, 386.
10. E. Aghaei, M. Haghighi, *Powder Technol.*, **2015**, *269*, 358.
11. M. Nikazar, K. Gholivand, K. Mahanpoor, *Kinet. Catal.*, **2007**, *48*, 214.
12. J.M. Wu, T.W. Zhang, *J. Photochem. Photobiol. A.*, **2004**, *162*, 171.
13. E. Pipelzadeh, A.A. Babaluo, M. Haghighi, A. Tavakoli, M. Valizadeh Derakhshan, A. Karimzadeh Behnami, *Chem. Eng. J.*, **2009**, *155*, 660.
14. Y.X. Yang, M.L. Liu, H. Zhu, Y.R. Chen, G.J. Mu, X.N. Liu, Y.Q. Jia, *J. Magn. Magn. Mater.*, **2008**, *320*, L132.
15. N.K. Chaudhari, H.C. Kim, D. Son, J.-S. Yu, *Cryst. Eng. Comm.*, **2009**, *11*, 2264.
16. E. Aghaei, M. Haghighi, *Powder Technol.*, **2015**, *269*, 358.